IMA Journal of Applied Mathematics (2024) **89**, 989–1005
https://doi.org/10.1093/imamat/hxaf005
Advance Access publication on 21 March 2025

Stability of smooth solitary waves under intensity-dependent dispersion

P. G. Kevrekidis
Department of Mathematics and Statistics, University of Massachusetts, Amherst, MA 01003-4515, USA

D. E. Pelinovsky
Department of Mathematics and Statistics, McMaster University, Hamilton, Ontario L8S 4K1, Canada

AND

R. M. Ross*
Department of Mathematics and Statistics, University of Massachusetts, Amherst, MA 01003-4515, USA
*Corresponding author: rmross@umass.edu

[Received on 22 August 2024; revised on 18 February 2025; accepted on 10 March 2025]

The nonlinear Schrödinger (NLS) equation in one dimension is considered in the presence of an intensity-dependent dispersion term. We study bright solitary waves with smooth profiles that extend from the limit where the dependence of the dispersion coefficient on the wave intensity is negligible to the limit where the solitary wave becomes singular due to vanishing dispersion coefficient. We analyse and numerically explore the stability for such smooth solitary waves, showing with the help of numerical approximations that the family of solitary waves becomes unstable in an intermediate region between the two limits, while being stable in both limits. This bistability, which has also been observed in other NLS equations with generalized nonlinearity, brings about interesting dynamical transitions from one stable branch to another stable branch, which are explored in direct numerical simulations of the NLS equation with the intensity-dependent dispersion term.

Keywords: intensity-dependent dispersion; smooth solitons; energetic stability.

1. Introduction

The nonlinear Schrödinger (NLS) equation in one dimension is one of the basic models of nonlinear optics, photonics, physics of plasma and hydrodynamics (Fibich, 2015; Kevrekidis *et al.*, 2015). The cubic NLS equation can be modified by the inclusion of intensity-dependent dispersion (IDD) in the general form

$$i\partial_t \psi + d(|\psi|^2)\partial_x^2 \psi + \gamma |\psi|^2 \psi = 0, \tag{1}$$

where γ is the coefficient of the Kerr nonlinearity, $d : (0, \infty) \to \mathbb{R}$ is the IDD coefficient and $\psi = \psi(t, x)$ is the wave function in $(t, x) \in \mathbb{R} \times \mathbb{R}$. If $d(|\psi|^2) = 1$, then the cubic NLS equation (1) is focusing for $\gamma > 0$ and defocusing for $\gamma < 0$. It admits bright solitons at the zero background in the former case and dark solitons at the non-zero background in the latter case.

The NLS equation with non-constant $d(|\psi|^2)$ has been used in physics literature to model coherently prepared multistate atoms (Greentree *et al.*, 2003), quantum well waveguides (Koser *et al.*, 2009),

fibre-optics communication systems (Lin *et al.*, 2020) and quantum harmonic oscillators in the presence of nonlinear effective masses (Chang *et al.*, 2022). The dispersion coefficient $d(|\psi|^2)$ may both decrease and increase with respect to the light intensity (Greentree *et al.*, 2003). Both cases can be modelled in a prototypical form through the dependence $d(|\psi|^2) = 1 - b|\psi|^2$ with b being either positive or negative constant parameter (Lin *et al.*, 2020).

The mathematical study of the intensity-dependent NLS models started with Ross *et al.* (2021), where we addressed the model (1) with $d(|\psi|^2) = 1 - b|\psi|^2$ and $\gamma = 0$. We proved that no bright solitary waves exist for $b < 0$ and a continuous family of bright solitary waves with singular profiles exist for $b > 0$. The continuous family can be parameterized by the distance between the two singularities where the wave profile is bounded and the derivative is unbounded. Energetic stability of the entire family of singular solitary waves was proven in Pelinovsky *et al.* (2021) by using minimization of the mass functional at fixed energy and fixed distance between the two singularities. The stability was obtained for perturbations to the soliton profile in the Sobolev space $H^1(\mathbb{R})$ within a weak formulation with the fixed distance between the two singularities.

Another relevant study was done in Pelinovsky & Plum (2024a), where dark solitary waves were obtained in the case $d(|\psi|^2) = 1/(1 - |\psi|^2)$ and $\gamma = 0$. The profiles of dark solitary waves are smooth, but the time evolution of the NLS equation is singular. In the particular case of the black solitary waves, it was shown in Pelinovsky & Plum (2024a) that the stability spectrum consists of isolated eigenvalues and no continuous spectrum. Similar stability studies of bright and dark solitary waves were performed in Albert & Arbunich (2024); Pelinovsky & Plum (2024b) for the regularized NLS equation proposed earlier in Dumas *et al.* (2016) and studied in Antonelli *et al.* (2019). It was suggested in Pelinovsky & Plum (2024b) that one can combine the IDD term from Pelinovsky & Plum (2024a) and the regularization term from Dumas *et al.* (2016) into the unified model given by the modified NLS equation.

Here we consider a different unified model, where the IDD term from Ross *et al.* (2021) is combined with a Kerr cubic focusing term. In other words, we address the NLS-IDD equation in the form

$$i\partial_t\psi + (1 - |\psi|^2)\partial_x^2\psi + \gamma|\psi|^2\psi = 0, \tag{2}$$

with $\gamma > 0$. Setting $\gamma = 0$ recovers the original IDD model considered in Pelinovsky *et al.* (2021); Ross *et al.* (2021). Hereafter we normalize $\gamma = 1$, which can be done without loss of generality since the scaling transformation $(t, x) \mapsto (t/\gamma, x/\sqrt{\gamma})$ generates the corresponding solutions of the NLS-IDD equation (2) with arbitrary $\gamma > 0$.

The NLS-IDD equation (2) is of interest in its own right as a setting presenting the competition of the above-mentioned IDD terms with the standard cubic nonlinearity of relevance to optical and atomic systems (Kivshar & Agrawal, 2003; Pitaevskii & Stringari, 2003). Additionally, it is also of interest as a continuum limit of the well-known Salerno model first proposed in Salerno (1992). The latter has been used extensively for exploring the breaking of integrability, evolution of conserved quantities and dynamics of solitary waves, among many other topics (Cai *et al.*, 1995; Mithun *et al.*, 2023). The Salerno model is written as the lattice differential equation

$$i\partial_t\psi_n + (1 - |\psi_n|^2)(\psi_{n+1} + \psi_{n-1}) + \mu|\psi_n|^2\psi_n = 0, \tag{3}$$

where $\mu \in \mathbb{R}$ is the coefficient of the onsite nonlinearity, $\psi_n = \psi_n(t)$ is the wave function in $(t, n) \in \mathbb{R}\times\mathbb{Z}$ and we have normalized the coefficient of the intersite nonlinearity to unity. In the continuum limit where $\psi_n(t) = \mathrm{e}^{2it}\psi(h^2t, hn)$ with small stepsize h and smooth $\psi = \psi(t, x)$, we can pick $\mu = 2 + h^2\gamma$ and obtain (2) from (3) at the truncated order $\mathcal{O}(h^2)$. Hence, the NLS-IDD equation (2) also describes the continuum dynamics of the Salerno model with competing onside and intersite nonlinearities.

We rewrite the NLS-IDD equation (2) with $\gamma = 1$ as

$$i\partial_t\psi + (1 - |\psi|^2)\partial_x^2\psi + |\psi|^2\psi = 0. \tag{4}$$

Similarly to other NLS equations with IDD terms, the NLS-IDD equation (4) is a Hamiltonian system with three basic conserved quantities given by energy

$$H(\psi) = \int_{\mathbb{R}} |\partial_x\psi|^2 + |\psi|^2 + \log(1 - |\psi|^2)\,\mathrm{d}x, \tag{5}$$

mass

$$Q(\psi) = -\int_{\mathbb{R}} \log(1 - |\psi|^2)\,\mathrm{d}x \tag{6}$$

and momentum

$$P(\psi) = i\int_{\mathbb{R}} \frac{\bar\psi\partial_x\psi - \psi\partial_x\bar\psi}{|\psi|^2}\,\mathrm{d}x, \tag{7}$$

where $H(\psi)$ and $Q(\psi)$ are well defined in the set of functions

$$\mathcal{X} := \left\{\psi \in H^1(\mathbb{R}) : \quad \|\psi\|_{L^\infty} < 1\right\} \tag{8}$$

and $P(\psi)$ is well defined for any solution for which $\psi(x) \neq 0$ for all $x \in \mathbb{R}$.

The energy, mass and momentum are conserved in the time evolution of the NLS-IDD equation (4) due to the translational and phase symmetries given by

$$\psi(t, x) \mapsto \psi(t + t_0, x + x_0)\,\mathrm{e}^{i\theta_0}, \quad t_0, x_0, \theta_0 \in \mathbb{R}. \tag{9}$$

Conservation of $H(\psi)$ in (5) follows from writing (4) in the Hamiltonian form

$$i\partial_t\psi = (1 - |\psi|^2)\frac{\delta H}{\delta\bar\psi}, \qquad \frac{\delta H}{\delta\bar\psi} = -\partial_x^2\psi - \frac{|\psi|^2\psi}{1 - |\psi|^2},$$

from which we obtain

$$\frac{\mathrm{d}}{\mathrm{d}t}H(\psi) = \int_{\mathbb{R}} \left(\frac{\delta H}{\delta\bar\psi}\partial_t\psi + \frac{\delta H}{\delta\bar\psi}\partial_t\bar\psi\right)\mathrm{d}x = 0.$$

Conservation of $Q(\psi)$ in (6) follows from the balance equation

$$i\partial_t \log(1 - |\psi|^2) = \partial_x\left(\bar\psi\partial_x\psi - \psi\partial_x\bar\psi\right),$$

which is obtained from (4).

Conservation of $P(\psi)$ in (7) can be checked directly as

$$\frac{\mathrm{d}}{\mathrm{d}t}P(\psi) = \int_{\mathbb{R}} \left(\frac{\partial_x \psi \partial_x^2 \psi}{\psi^2} - \frac{\partial_x^3 \psi}{\psi} + \frac{\partial_x \bar{\psi} \partial_x^2 \bar{\psi}}{\bar{\psi}^2} - \frac{\partial_x^3 \bar{\psi}}{\bar{\psi}} \right) \mathrm{d}x$$
$$+ \int_{\mathbb{R}} \left(\bar{\psi} \partial_x^3 \psi + \partial_x \bar{\psi} \partial_x^2 \psi + \psi \partial_x^3 \bar{\psi} + \partial_x \psi \partial_x^2 \bar{\psi} \right) \mathrm{d}x$$
$$- 2 \int_{\mathbb{R}} \partial_x |\psi|^2 \mathrm{d}x = 0.$$

The momentum $P(\psi)$ corresponds to the renormalized momentum, which is the only momentum-type conserved quantity in the NLS equation with IDD terms, see Pelinovsky & Plum (2024a).

Bright solitons of the NLS-IDD equation (4) are standing wave solutions of the form

$$\psi(x,t) = \mathrm{e}^{i\omega t} \varphi_\omega(x)$$

with the frequency $\omega > 0$ and the profile φ_ω being a real, spatially decaying solution of the second-order differential equation

$$\frac{\mathrm{d}^2 \varphi}{\mathrm{d}x^2} = \frac{(\omega - \varphi^2)}{1 - \varphi^2} \varphi = -\frac{\mathrm{d}V}{\mathrm{d}\varphi} \tag{10}$$

associated with the potential energy

$$V(\varphi) := \frac{\omega - 1}{2} \log |1 - \varphi^2| - \frac{1}{2} \varphi^2. \tag{11}$$

The existence of bright solitons with smooth profiles φ_ω is given by the following theorem.

THEOREM 1. The second-order profile equation (10) admits a unique smooth solitary wave solution $\varphi_\omega \in H^\infty(\mathbb{R})$ if and only if $\omega \in (0,1)$. Moreover, the family $\{\varphi_\omega\}_{\omega \in (0,1)}$ is smooth with respect to ω.

REMARK 1. In the limit $\omega \to 0$, the size of φ_ω is small according to the formal asymptotic expansion

$$\varphi_\omega(x) = \varepsilon \phi_\Omega(\varepsilon x) + \mathcal{O}(\varepsilon^3), \qquad \omega = \varepsilon^2 \Omega,$$

where the profile ϕ_Ω is found from the second-order equation

$$\phi'' = \Omega \phi - \phi^3$$

for every fixed $\Omega > 0$. It is available in the explicit form

$$\phi_\Omega(x) = \sqrt{2\Omega}\, \mathrm{sech}(\sqrt{\Omega} x).$$

In the limit $\omega \to 1$, the second-order equation (10) becomes linear, i.e. $\varphi'' = \varphi$, with the formal peakon solution

$$\varphi_{\omega=1}(x) = \mathrm{e}^{-|x|}.$$

The case $\omega > 1$ gives a family of bright solitons with singular profiles whose singularities are the same as in Pelinovsky *et al.* (2021); Ross *et al.* (2021).

The main motivation for our work is to establish the energetic stability of bright solitons with smooth profiles φ_ω for $\omega \in (0, 1)$ under the presence of IDD. The following theorem presents the main result.

THEOREM 2. Let $\varphi_\omega \in H^\infty(\mathbb{R})$ be the spatial profile satisfying (10) for $\omega \in (0, 1)$, according to Theorem 1. Then, it is a local non-degenerate (up to two symmetries) minimizer of the augmented energy $\Lambda_\omega := H + \omega Q$ subject to fixed mass Q in $H^1(\mathbb{R})$ if and only if the mapping $\omega \mapsto Q(\varphi_\omega)$ is monotonically increasing.

REMARK 2. If local well-posedness of the NLS-IDD equation (4) can be established in the function set $\mathcal{X}$ in (8), then Theorem 2 yields the orbital stability of bright solitons along the orbit $\{\varphi_\omega(\cdot - \xi)\mathrm{e}^{i\theta}\}_{\xi,\theta\in\mathbb{R}}$ in $H^1(\mathbb{R})$. However, local well-posedness for quasilinear NLS equations of the class (4) is known only in Sobolev spaces of higher regularity (Poppenberg, 2001; Kenig *et al.*, 2004; Feola *et al.*, 2023), e.g. in $H^s(\mathbb{R})$ for $s > 2$ (Marzuola *et al.*, 2021) and for small data in $H^s(\mathbb{R})$ for $s > 1$ (Ifrim & Tataru, 2023).

REMARK 3. We show numerically that there exist ω_1, ω_2 satisfying $0 < \omega_1 < \omega_2 < 1$ such that the mapping $\omega \mapsto Q(\varphi_\omega)$ is monotonically increasing if $\omega \in (0, \omega_1) \cup (\omega_2, 1)$ and monotonically decreasing if $\omega \in (\omega_1, \omega_2)$. The bright soliton with profile φ_ω is energetically stable in the former case and energetically unstable in the latter case. In the limits $\omega \to 0$ and $\omega \to 1$ our results are in agreement with the stability of bright solitons in the cubic NLS equation, as well as the energetic stability of singular solitary waves in the NLS-IDD equation (4) with $\gamma = 0$, which was proven in Pelinovsky *et al.* (2021).

REMARK 4. The spectral instability of solitary waves for $\omega \in (\omega_1, \omega_2)$ has also been observed in various models involving a modification of the standard dispersion and cubic nonlinearity. Such examples include discrete NLS equations with long-range dispersion (Johansson *et al.*, 1998) and power nonlinearity (Malomed & Weinstein, 1996), as well as the generalized NLS equations with competing power nonlinearities (Pelinovsky *et al.*, 1996).

The paper is organized as follows. Existence of the bright solitons with smooth profiles is considered in Section 2 with phase plane analysis, where the proof of Theorem 1 is given. The proof of Theorem 2 regarding stability of the bright solitons is developed in Section 3, with analysis of the Hessian operator for the augmented energy $\Lambda_\omega = H + \omega Q$. Numerical results are described in Section 4, where we approximate the mapping $\omega \mapsto Q(\varphi_\omega)$, eigenvalues of the spectral stability problem and the time-dependent evolution of the NLS equation (4) suggesting that spectrally stable bright solitons are also dynamically (nonlinearly) stable. An outlook of open directions of study is given in Section 5.

2. Existence of bright solitons with smooth profiles

Here we consider solutions of the second-order equation (10) on the phase plane $(\varphi, \varphi') \in \mathbb{R}^2$. First we consider the case $\omega > 0$, for which there exist three local extrema of the potential V at $\varphi = 0$ and

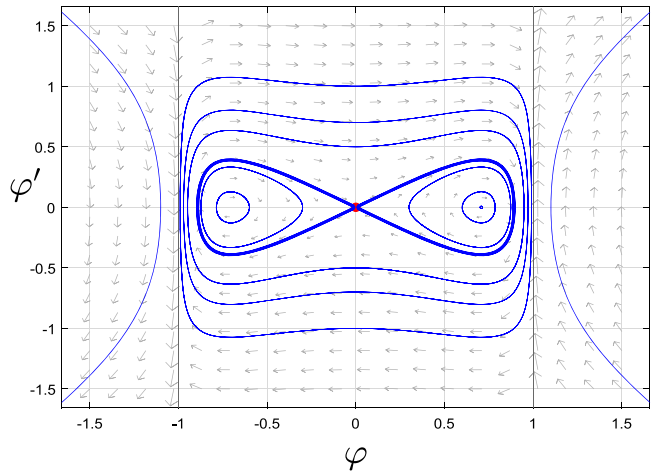

FIG. 1. Phase portrait for the second-order equation (10) with $\omega \in (0,1)$. Two homoclinic orbits correspond to the smooth profiles $\pm\varphi_\omega$ with values in $(-1,1)$.

$\varphi = \pm\sqrt{\omega}$ as well as two singularities at $\varphi = \pm 1$; see (11). We denote $\varphi_* := \sqrt{\omega}$. Since

$$V''(\varphi) = -\frac{\omega(1+\varphi^2) + \varphi^2(\varphi^2 - 3)}{(1-\varphi^2)^2},$$

we obtain

$$V''(\varphi_*) = \frac{2\omega}{\omega - 1}.$$

Hence $\pm\varphi_*$ are minima of V for $\omega \in (0,1)$ and maxima of V for $\omega \in (1,\infty)$, whereas 0 is always a maximum of V if $\omega > 0$. Different cases are considered next.

(1) $\omega \in (0,1)$. Since $\varphi_* \in (0,1)$, there are three equilibrium points in the vertical strip $(\varphi,\varphi') \in [-1,1]\times\mathbb{R}$. The origin $(0,0)$ is a saddle point and $(\pm\varphi_*,0)$ are centre points, since V is similar to a double-well potential in $[-1,1]$ with $V(\varphi) \to +\infty$ as $\varphi \to \pm 1$. The phase portrait of the planar Hamiltonian system described by the second-order equation (10) is shown on Fig. 1 from the level curves of the function

$$E(\varphi,\varphi') := \frac{1}{2}(\varphi')^2 + V(\varphi),$$

which is x-independent on every smooth solution of (10). Periodic orbits exist in the vertical strip $[-1,1]\times\mathbb{R}$ for every $E \in (V(\varphi_*),0)\cup(0,\infty)$ either inside or outside the homoclinic orbits for $E = 0$. The homoclinic orbit with $E = 0$ corresponds to the smooth profile $\varphi_\omega \in H^\infty(\mathbb{R})$ of Theorem 1. Its maximum value is the unique solution $\varphi_0 \in (0,1)$ of $V(\varphi) = 0$. All orbits outside $[-1,1]\times\mathbb{R}$ diverge to infinity. Since V is smooth with respect to ω and φ_ω is bounded away from 1 for every $\omega \in (0,1)$, the spatial profile φ_ω is smooth with respect to ω. Examples

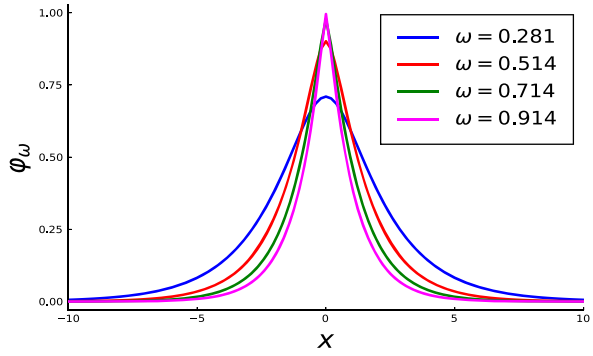

FIG. 2. Bright soliton profiles φ_ω for various values of the frequency ω.

of the smooth profiles φ_ω are shown on Fig. 2. The slopes grow as the values of ω increase towards 1.

(2) $\underline{\omega = 1.}$ The singularity is cancelled for the potential $V(\varphi) = -\frac{1}{2}\varphi^2$ and all smooth solutions of the linear equation $\varphi'' = \varphi$ diverge to infinity. However, there exists a formal peakon solution with the profile $\varphi_{\omega=1} \in H^1(\mathbb{R})$; see Remark 1.

(3) $\underline{\omega \in (1, \infty).}$ Since $\pm\varphi_*$ are now maxima of V outside $[-1, 1]$, we have $V(\varphi) \to -\infty$ as $\varphi \to \pm 1$. The other maximum is at 0 with $V(0) = 0$, so we compute

$$V_*(\omega) := V(\varphi_*) = \frac{\omega - 1}{2} \log(\omega - 1) - \frac{\omega}{2}, \qquad \text{for } \omega \in (1, \infty).$$

This function has a unique zero $\omega = \omega_* > 1$, such that $V_*(\omega_*) = 0$ and $V_*(\omega) \lessgtr 0$ for $\omega \lessgtr \omega_*$; see Fig. 3.

The phenomenology for $\omega > 1$ is now further subdivided into the cases $\omega \in (1, \omega_*)$ and $\omega \in (\omega_*, \infty)$, with the only difference between them being the behaviour of smooth orbits at the level $E = 0$ outside of the strip $[-1, 1] \times \mathbb{R}$. Figure 4 shows the relevant phase portraits of the second-order equation (10) for the two cases. In both cases, all smooth solutions of (10) diverge to infinity, and the homoclinic orbits for the level $E = 0$ are broken at the singularities at $\varphi = \pm 1$. Outside of the vertical strip $[-1, 1] \times \mathbb{R}$, the smooth orbits at the same level $E = 0$ either diverge to infinity for $\omega \in (1, \omega_*)$, or are bounced back to the singularities at $\varphi = \pm 1$ for $\omega \in (\omega_*, \infty)$. The latter case resembles the one in Ross *et al.* (2021), where we constructed a continuous family of bell-shaped solitary waves with singular profiles within a weak formulation of the second-order equation (10) in the absence of the cubic term.

For $\omega \leq 0$, there is only one local extremum of V at 0, which is a local minimum, and $V(\varphi) \to +\infty$ as $\varphi \to \pm 1$. Smooth orbits of the second-order equation (10) are periodic inside the vertical strip $[-1, 1] \times \mathbb{R}$ and unbounded outside the strip. There are no homoclinic orbits for $\omega \leq 0$.

Based on the above analysis, the proof of Theorem 1 is complete.

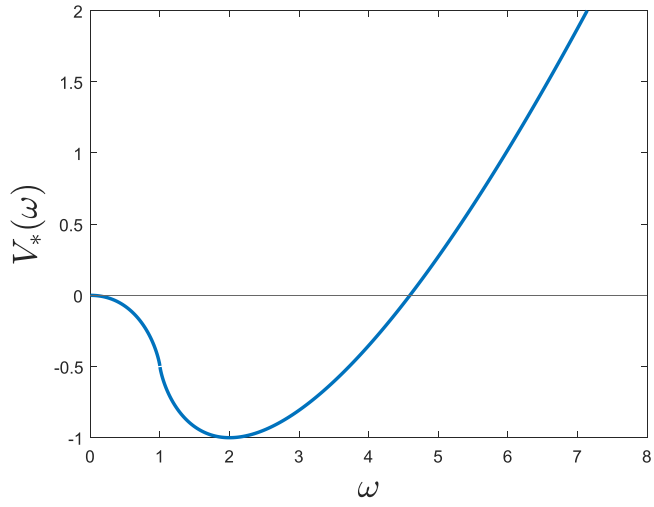

FIG. 3. The function $V_*(\omega)$ vs. ω. The unique zero of V_* for positive ω occurs at $\omega = \omega_*$.

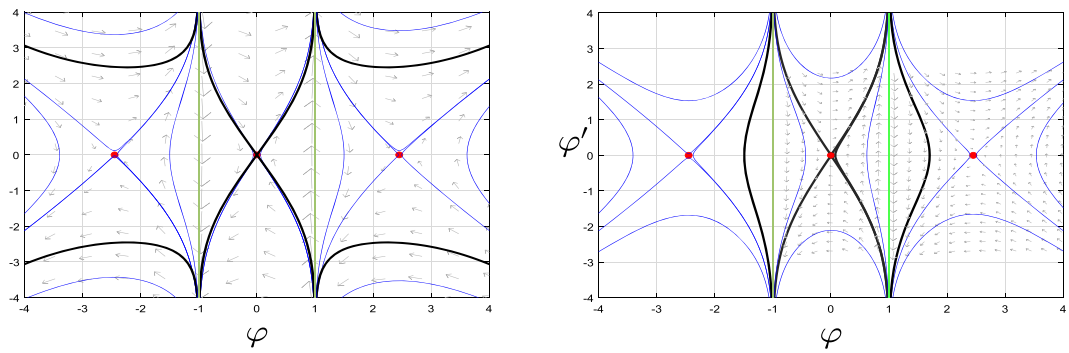

FIG. 4. Phase portraits for the second-order equation (10). Since we found numerically that $\omega_* \approx 4.5$, we use $\omega = 3$ for the case $\omega \in (1, \omega_*)$ (left), and $\omega = 6$ for $\omega \in (\omega_*, \infty)$ (right). In both panels, the green vertical lines indicate the singularities at $\varphi = \pm 1$, and the black curves are the level curves for $E(\varphi, \varphi') = 0$.

3. Stability of bright solitons with smooth profiles

Let $\varphi_\omega \in H^\infty(\mathbb{R})$ be the spatial profile satisfying (10) for $\omega \in (0, 1)$, according to Theorem 1. Adding a perturbation $u + iv$ to the profile φ_ω and linearizing yields the spectral stability problem in the form

$$\begin{pmatrix} 0 & \mathcal{L}_- \\ -\mathcal{L}_+ & 0 \end{pmatrix} \begin{pmatrix} u \\ v \end{pmatrix} = \lambda \begin{pmatrix} u \\ v \end{pmatrix}, \tag{12}$$

where

$$\mathcal{L}_- := -(1 - \varphi_\omega^2)\partial_x^2 + \omega - \varphi_\omega^2,$$
$$\mathcal{L}_+ := -(1 - \varphi_\omega^2)\partial_x^2 + \omega + 2\varphi_\omega \partial_x^2 \varphi_\omega - 3\varphi_\omega^2.$$

Since the coefficient $(1-\varphi_\omega^2)$ is sign-definite for the profile $\varphi_\omega \in H^\infty(\mathbb{R})$ of Theorem 1, the weight $(1-\varphi_\omega^2)^{-1}$ is bounded away from 0 and converges to 1 as $|x| \to \infty$. The linear Schrödinger operators

$$\mathcal{S}_\pm := (1-\varphi_\omega^2)^{-1}\mathcal{L}_\pm : H^2(\mathbb{R}) \subset L^2(\mathbb{R}) \to L^2(\mathbb{R}) \tag{13}$$

are self-adjoint so that we can consider the spectral stability problem (12) in the weighted Hilbert space $\mathcal{H}\times\mathcal{H}$, where $\mathcal{H} := L^2(\mathbb{R}, (1-\varphi_\omega^2)^{-1}\,dx)$ is equipped with the inner product

$$\langle \cdot,\cdot\rangle_{\mathcal{H}} := \langle (1-\varphi_\omega^2)^{-1}\cdot,\cdot\rangle_{L^2}.$$

This approach is very similar to the study of stability in the regularized NLS equation, see Pelinovsky & Plum (2024a). Since $(1-\varphi_\omega^2)$ is bounded away from 0, we can reformulate the spectral stability problem (12) in the equivalent form

$$\begin{pmatrix} 0 & \mathcal{M}_- \\ -\mathcal{M}_+ & 0 \end{pmatrix}\begin{pmatrix} \tilde{u} \\ \tilde{v} \end{pmatrix} = \lambda \begin{pmatrix} \tilde{u} \\ \tilde{v} \end{pmatrix}, \tag{14}$$

where $(\tilde{u},\tilde{v}) = (1-\varphi_\omega^2)^{-1/2}(u,v)$ and

$$\mathcal{M}_\pm := (1-\varphi_\omega^2)^{1/2}\mathcal{S}_\pm(1-\varphi_\omega^2)^{1/2} : H^2(\mathbb{R}) \subset L^2(\mathbb{R}) \to L^2(\mathbb{R}) \tag{15}$$

are also self-adjoint operators.

For the proof of the energetic stability of bright solitons with smooth profiles φ_ω, we follow the standard algorithm of placing φ_ω in the variational context as a critical point of the augmented energy $\Lambda_\omega := H + \omega Q$, where H and Q are given by (5) and (6), respectively. Then, we show that $\mathcal{S}_\pm$ in (13) are Hessian operators of the variational problem and that their combined spectra in $L^2(\mathbb{R})$ includes a simple negative eigenvalue, a double zero eigenvalue and a strictly positive part bounded away from zero. Finally, we show that φ_ω is a local non-degenerate (up to two symmetries) minimizer of Λ_ω subject to fixed mass Q if and only if the mapping $\omega \mapsto Q(\varphi_\omega)$ is monotonically increasing. This yields the criterion for energetic stability of the bright solitons with smooth profiles φ_ω given by Theorem 2.

For a linear operator $T : \mathcal{D}(T) \subset \mathcal{H} \to \mathcal{H}$ with a dense domain $\mathcal{D}(T)$ in a Hilbert space $\mathcal{H}$, we denote

$$n(T) = \dim\{v \in \mathcal{H} : \quad \langle Tv, v\rangle_{\mathcal{H}} < 0\},$$

which is the combined multiplicity of all negative eigenvalues of T. Similarly, we denote the multiplicity of the zero eigenvalue of T by $z(T)$. The algorithm of the proof of Theorem 2 is divided into several steps.

Step 1: φ_ω is a solution of the Euler–Lagrange equation for $\Lambda_\omega = H + \omega Q$.

To derive the Euler-Lagrange equation, we compute the variational derivatives of H and Q with respect to $\bar{\psi}$:

$$\frac{\delta H}{\delta\bar{\psi}} = -\partial_x^2\psi - \frac{|\psi|^2\psi}{1-|\psi|^2}, \qquad \frac{\delta Q}{\delta\bar{\psi}} = \frac{\psi}{1-|\psi|^2},$$

so that the second-order equation (10) is written as

$$\frac{\delta H}{\delta \bar{\psi}} + \omega \frac{\delta Q}{\delta \bar{\psi}} = 0.$$

Hence, φ_ω is a critical point of Λ_ω.

Step 2: The operators $\mathcal{S}_\pm$ in (13) are the Hessian operators of Λ_ω at φ_ω.

For Step 2, we add a perturbation $u + iv$ to φ_ω and use Step 1 to derive the expansion

$$\Lambda_\omega(\varphi_\omega + u + iv) - \Lambda_\omega(\varphi_\omega) = \langle \mathcal{S}_+ u, u\rangle_{L^2} + \langle \mathcal{S}_- v, v\rangle_{L^2} + \mathcal{O}\left(\|u + iv\|_{H^1}^3\right),$$

where $\mathcal{S}_\pm$ are given by (13). Hence, $\mathcal{S}_\pm$ are Hessian operators of Λ_ω at φ_ω.

Step 3: $n(\mathcal{S}_-) = 0$ and $z(\mathcal{S}_-) = 1$ in $L^2(\mathbb{R})$.

To prove Step 3, we recall that $\mathcal{S}_- = (1 - \varphi_\omega^2)^{-1}\mathcal{L}_-$. Due to phase rotation symmetry, we have $\mathcal{L}_-\varphi_\omega = 0$ with $\varphi_\omega(x) > 0$ and $\varphi_\omega \in H^2(\mathbb{R})$. The essential spectrum of $\mathcal{S}_-$ in $L^2(\mathbb{R})$ is given by $[\omega, \infty)$ by Weyl's theorem. Since the essential spectrum is bounded away from zero by the positive constant $\omega > 0$, and φ_ω is strictly positive, Sturm's comparison theorem implies that $n(\mathcal{S}_-) = 0$ and $z(\mathcal{S}_-) = 1$.

Step 4: $n(\mathcal{S}_+) = 1$ and $z(\mathcal{S}_+) = 1$ in $L^2(\mathbb{R})$.

To prove Step 4, we recall that $\mathcal{S}_+ = (1 - \varphi_\omega^2)^{-1}\mathcal{L}_+$. Due to spatial translation symmetry, we have $\mathcal{L}_+\partial_x\varphi_\omega = 0$ with $\partial_x\varphi_\omega \in H^2(\mathbb{R})$ having exactly one zero on $\mathbb{R}$. Since

$$\omega + 2\varphi_\omega\partial_x^2\varphi_\omega - 3\varphi_\omega^2 = \omega\frac{1 + \varphi_\omega^2}{1 - \varphi_\omega^2} - \varphi_\omega^2\frac{3 - \varphi_\omega^2}{1 - \varphi_\omega^2}, \tag{16}$$

and $\varphi_\omega(x) \to 0$ as $|x| \to \infty$ exponentially fast, the essential spectrum of $\mathcal{S}_+$ in $L^2(\mathbb{R})$ is given by $[\omega, \infty)$ by Weyl's theorem. Since again the essential spectrum is bounded away from zero by the positive constant $\omega > 0$, a single zero of $\partial_x\varphi_\omega$ on $\mathbb{R}$ implies by Sturm's comparison theorem that $n(\mathcal{S}_-) = 1$ and $z(\mathcal{S}_-) = 1$.

Step 5: φ_ω is a local non-degenerate (up to two symmetries) minimizer of Λ_ω subject to fixed mass Q if and only if the mapping $\omega \mapsto Q(\varphi_\omega)$ is monotonically increasing.

To prove Step 5, we need to show $n(\mathcal{S}_+|_{\{v_\omega\}^\perp}) = 0$ and $z(\mathcal{S}_+|_{\{v_\omega\}^\perp}) = 1$, where

$$v_\omega := \frac{\varphi_\omega}{1 - \varphi_\omega^2}$$

represents the first variation of Q at φ_ω as in Step 1 and $\mathcal{S}_+|_{\{v_\omega\}^\perp}$ denotes the restriction of $\mathcal{S}_+$ to the constrained $L^2(\mathbb{R})$ space with the scalar orthogonality condition $\langle \cdot, v_\omega\rangle_{L^2} = 0$. As is well known, if $n(\mathcal{S}_+) = 1$, $n(\mathcal{S}_-) = 0$ and $z(\mathcal{S}_\pm) = 1$ as in Steps 3 and 4 and $\mathcal{S}_\pm$ are Hessian operators for Λ_ω at φ_ω as in Step 2, then the assertion is true if and only if

$$\langle \mathcal{S}_+^{-1} v_\omega, v_\omega\rangle_{L^2} < 0.$$

Recall by Theorem 1 that $\varphi_\omega \in H^\infty(\mathbb{R})$ is also smooth with respect to ω for $\omega \in (0,1)$. By differentiating equation (10) in ω for $\omega \in (0,1)$ and comparing with (16), we get

$$\mathcal{S}_+ \partial_\omega \varphi_\omega = -v_\omega.$$

Hence

$$\langle \mathcal{S}_+^{-1} v_\omega, v_\omega \rangle_{L^2} = -\langle \partial_\omega \varphi_\omega, v_\omega \rangle_{L^2} = -\frac{1}{2} \partial_\omega Q(\varphi_\omega),$$

and the assertion is true if and only if the mapping $\omega \mapsto Q(\varphi_\omega)$ is monotonically increasing.

Based on the above five steps, the proof of Theorem 2 is complete.

REMARK 5. If the bright soliton with profile φ_ω is a local non-degenerate (up to two symmetries) minimizer of Λ_ω subject to fixed mass Q as in Theorem 2, then the linear spectral problem

$$\begin{pmatrix} 0 & \mathcal{S}_- \\ -\mathcal{S}_+ & 0 \end{pmatrix} \begin{pmatrix} u \\ v \end{pmatrix} = \lambda \begin{pmatrix} u \\ v \end{pmatrix}$$

admits no eigenvalues $\lambda \in \mathbb{C} \backslash \{i\mathbb{R}\}$ with eigenvectors $(u, v) \in H^2(\mathbb{R}) \times H^2(\mathbb{R})$. Since the weight $(1 - \varphi_\omega^2)^{-1/2}$ is bounded away from 0 and ∞, Sylvester's inertia law implies the same counts of negative and zero eigenvalues of $\mathcal{M}_\pm$ in L^2 for $\mathcal{M}_\pm$ given by (15). This implies the same stability result in the spectral problem (14). Finally, by the same boundedness of $(1 - \varphi_\omega^2)^{-1/2}$ and the transformation of the eigenvector $(u, v) \in H^2(\mathbb{R}) \times H^2(\mathbb{R})$ to $(\tilde{u}, \tilde{v}) \in H^2(\mathbb{R}) \times H^2(\mathbb{R})$, this implies that $n(\mathcal{L}_+) = 1, n(\mathcal{L}_-) = 0$ and $z(\mathcal{L}_\pm) = 1$ in $\mathcal{H}$ and the same stability result holds in the spectral problem (12).

4. Numerical results

Here we illustrate numerically the statements in Theorem 2 and Remark 3, regarding monotonicity changes in the mapping $\omega \mapsto Q(\varphi_\omega)$ and spectral stability of bright solitons in the stability problem (12). In addition, we perform several numerical experiments that suggest that the spectrally stable solitons are also dynamically stable.

The smooth profiles φ_ω of the bright solitons are obtained numerically in the full range $\omega \in (0,1)$ via a standard pseudo-arclength continuation, using the continuation package `BifurcationKit.jl` in Julia (Veltz, 2020). At each continuation step, the profile is obtained by the GMRES method with a diagonal (Jacobi) preconditioner.

According to Theorem 2, the bright soliton with smooth profile φ_ω is stable if and only if the mapping $\omega \mapsto Q(\varphi_\omega)$ is increasing. Numerical computations show that this function has two extrema at $\omega_1, \omega_2 \in (0,1)$. The former is seen to be a maximum, while the latter is a minimum, leading to two switches in the stability of the bright solitons. These are indicated by the two vertical lines in the bottom panel of Fig. 5.

These stability conclusions are corroborated by numerical computations of the spectrum for the stability problem (12). Figure 6 shows the spectrum for various values of ω near the first critical point $\omega = \omega_1 \approx 0.592$. The situation is reversed at the second crossing for $\omega = \omega_2 \approx 0.843$, with the same eigenvalue pair crossing from the real axis back to the imaginary axis as ω increases. The condition $\partial_\omega Q(\varphi_\omega) = 0$ is equivalent to a pair of eigenvalues crossing from the imaginary axis to the real axis (or

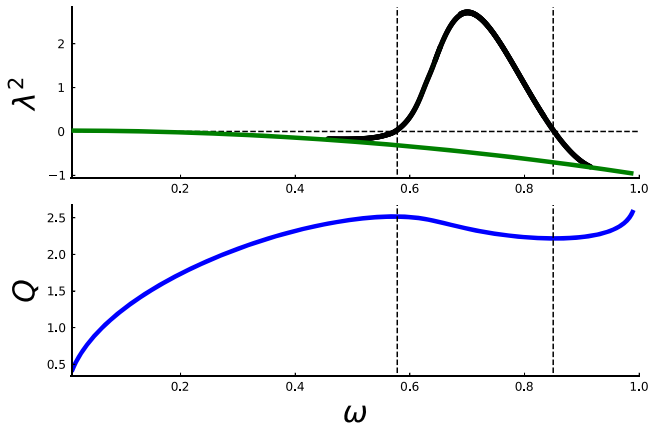

FIG. 5. Top: square of the bifurcating unstable eigenvalue λ^2 for the spectral stability problem (12). Bottom: the map $\omega \mapsto Q(\varphi_\omega)$. In the top panel, the dashed horizontal line is drawn at $\lambda^2 = 0$ and the solid green curve is the function $\omega \mapsto -\omega^2$, which is the boundary of the continuous spectrum. In both panels, the dashed vertical lines are drawn at ω_1 and ω_2.

vice versa) through the origin. Therefore we expect such eigenvalue zero-crossings at the critical points $\omega_1, \omega_2 \in (0,1)$ of the map $\omega \mapsto Q(\varphi_\omega)$. These are confirmed numerically, and are indicated by the vertical lines in the top panel of Fig. 5.

Let us now elaborate on the behaviour of eigenvalues for the spectral stability problem (12). From the symmetries in (9), we obtain two eigenvectors in the kernel of the stability problem (12):

$$\begin{pmatrix} 0 & \mathcal{L}_- \\ -\mathcal{L}_+ & 0 \end{pmatrix} \begin{pmatrix} \partial_x \varphi_\omega \\ 0 \end{pmatrix} = \begin{pmatrix} 0 \\ 0 \end{pmatrix} \qquad \text{and} \qquad \begin{pmatrix} 0 & \mathcal{L}_- \\ -\mathcal{L}_+ & 0 \end{pmatrix} \begin{pmatrix} 0 \\ \varphi_\omega \end{pmatrix} = \begin{pmatrix} 0 \\ 0 \end{pmatrix}.$$

The zero eigenvalue generally has quadruple algebraic multiplicity due to two generalized eigenvectors in the generalized kernel of the stability problem (12). To obtain the generalized eigenvectors, we consider a two-parameter family of standing and travelling wave solutions in the form

$$\psi(x,t) = \mathrm{e}^{i\omega t} \phi_{\omega,c}(x - ct),$$

where $\omega \in (0,1)$, $c \in (-c_0, c_0)$ for a small $c_0 > 0$, and the profile $\phi_{\omega,c}$ is a solution of the complex second-order equation

$$(1 - |\phi|^2)\phi'' + |\phi|^2 \phi = \omega\phi + ic\phi', \tag{17}$$

The profile $\varphi_\omega \equiv \psi_{\omega,c=0}$ has even parity, so that $\mathcal{S}_+ = (1 - \varphi_\omega^2)^{-1}\mathcal{L}_+$ is invertible on the subspace of even functions in $L^2(\mathbb{R})$ and $\mathcal{S}_- = (1 - \varphi_\omega^2)^{-1}\mathcal{L}_-$ is invertible on the subspace of odd functions in $L^2(\mathbb{R})$. As a result, the family $\{\phi_{\omega,c}\}_{\omega \in (0,1), c \in (-c_0,c_0)}$ of solutions of the second-order equation (17) is smooth for some $c_0 > 0$. Taking derivatives of (17) in ω and c, we obtain

$$\mathcal{L}_+ \partial_\omega \varphi_\omega = -\varphi_\omega, \qquad \mathcal{L}_- \partial_c \phi_{\omega,c}|_{c=0} = -\partial_x \varphi_\omega.$$

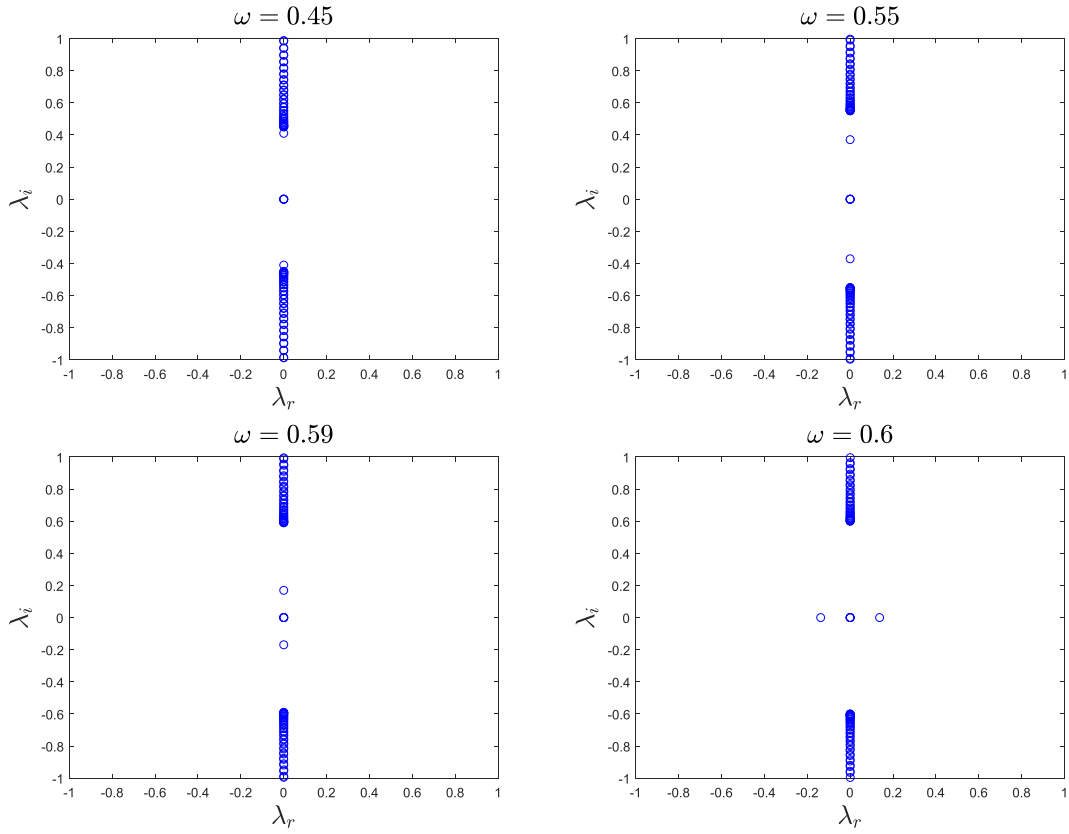

FIG. 6. Complex plane (λ_r, λ_i) for eigenvalues $\lambda = \lambda_r + i\lambda_i$ of the spectral stability problem (12), for ω values near the first eigenvalue crossing. As ω increases, the non-zero eigenvalue pair moves towards the origin, crossing through onto the real axis around $\omega_1 \approx 0.592$.

As a result, the generalized eigenvectors of the stability problem (12) are given by

$$\begin{pmatrix} 0 & \mathcal{L}_- \\ -\mathcal{L}_+ & 0 \end{pmatrix} \begin{pmatrix} 0 \\ -\partial_c \phi_{\omega,c}|_{c=0} \end{pmatrix} = \begin{pmatrix} \partial_x \varphi_\omega \\ 0 \end{pmatrix} \quad \text{and} \quad \begin{pmatrix} 0 & \mathcal{L}_- \\ -\mathcal{L}_+ & 0 \end{pmatrix} \begin{pmatrix} \partial_\omega \varphi_\omega \\ 0 \end{pmatrix} = \begin{pmatrix} 0 \\ \varphi_\omega \end{pmatrix}.$$

In addition to the quadruple zero eigenvalue and the continuous spectrum on

$$\{i\beta : \quad \beta \in (-\infty, -\omega] \cup [\omega, \infty)\},$$

the spectral problem (12) features a bifurcating eigenvalue pair that is responsible for the stability changes of the solitary waves.

This eigenvalue pair, shown in the top panel of Fig. 5 and also in Fig. 6, emerges from the continuous spectrum at $\omega \approx 0.443$ and moves along the imaginary axis towards the origin as ω increases, eventually crossing through to the real axis at $\omega = \omega_1 \approx 0.592$ and rendering the bright solitons unstable. The real eigenvalue pair later crosses back to the imaginary axis at $\omega = \omega_2 \approx 0.843$, and finally at $\omega \approx 0.912$ the

eigenvalue pair disappears into the continuous spectrum. The bright solitons are thus spectrally unstable for $\omega \in (\omega_1, \omega_2)$, and are spectrally stable for $\omega \in (0, \omega_1] \cup [\omega_2, 1)$.

Finally, we perform the following experiments to investigate the dynamical stability of bright solitons. Starting with an initial soliton φ_{ω_0} with $\omega_0 \in (0, 1)$, we make a small perturbation and evolve the solution up to a large time $T = 500$. The results shown here use generic Gaussian perturbations centred at the origin, but we have performed more experiments using different types of perturbations, including e.g. ones with sign changes, and the overall conclusions are the same as those below. We do not consider here the critical points ω_1 and ω_2 for which $\partial_\omega Q(\varphi_\omega) = 0$. Bright solitons for such critical cases are known to be nonlinearly unstable for generic Hamiltonian systems with $U(1)$ symmetry (Pelinovsky *et al.*, 1996; Comech & Pelinovsky, 2003).

If the perturbation to the bright soliton φ_{ω_0} is sufficiently small, we expect the solution to converge, up to radiation, to a stable bright soliton. Hence the solution is expected to be of the form

$$u(x, t) = \mathrm{e}^{i\omega_f t}\varphi_{\omega_f}(x) + (\text{radiation}), \tag{18}$$

for some final frequency ω_f. We now seek to confirm this conjecture.

After sufficient time has passed, the radiation will have dispersed significantly and will not play any role in the central region near $x = 0$. Therefore we measure the quantity $c(t) = \mathrm{Re}(u(0, t))$, which in view of (18) is expected to behave like $\cos(\omega_f t)$, and obtain its dominant frequency ω_f via the fast Fourier transform. Once ω_f is obtained, we match the spatial profile of the evolved final state $u_f(x)$ to the bright soliton $\varphi_{\omega_f}(x)$. We find good agreement between the two in all cases, confirming the decomposition (18).

In the case of small perturbations of the spectrally stable soliton, our computations indicate that the final frequency does not change much, i.e. $\omega_f \approx \omega_0$. This suggests that these bright solitons are also dynamically stable.

In the case of large perturbations, we have found that $\omega_f \neq \omega_0$ generically; nevertheless, the frequency ω_f lies on one of the stable branches. In particular, it is possible to transition between the two stable branches when a large perturbation is added. For spectrally unstable bright solitons, the perturbed solution always transforms to a state within the stable branches, confirming their dynamical instability.

Figure 7 summarizes in the (ω, Q) plane the outcomes of the transitions from A_0 and C_0 to either A_1 and C_1 or A_2 and C_2 in the case of large perturbations of the stable bright solitons, and the transitions from B_0 to either B_1 or B_2 in the case of small perturbations of the unstable bright solitons. The two transitions are defined by Gaussian perturbations of two different signs to the initial soliton profile φ_{ω_0}. Furthermore, details of the initial and final profiles are shown in Figs 8 and 9 (left panels) and the final nearly periodic oscillations of the soliton amplitude (right panels) for the transitions $B_0 \to B_1$ and $B_0 \to B_2$. Note that the final spatial profiles of the bright solitons at A_1, B_1 and C_1 are closer to the peaked profile at P, which occurs in the limit $\omega \to 1$.

5. Conclusion

In this work we have considered a new modification of the IDD models, where the nonlinearly modified dispersion competes with a local cubic nonlinearity. We argued that this model is of interest in its own right, but also emerges as a continuum limit of the Salerno model (3). By using the conservation laws and by analysing the stationary and spectral stability problems for this model, we showed that the bright solitons with smooth profiles exist if the frequency lies within a suitable parametric interval. We have obtained the stability criterion for such smooth bright solitons from the monotonic dependence of the mass on the frequency, in line with the well-known stability criterion in NLS-type models.

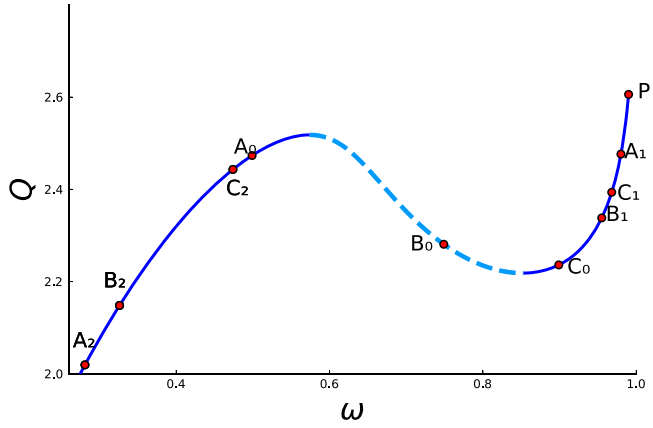

FIG. 7. Initial and final frequencies shown in the (ω, Q) plane for the numerical simulations. The point P represents the bright soliton with the peaked profile. The dashed line indicates the unstable branch, while the other two branches are stable.

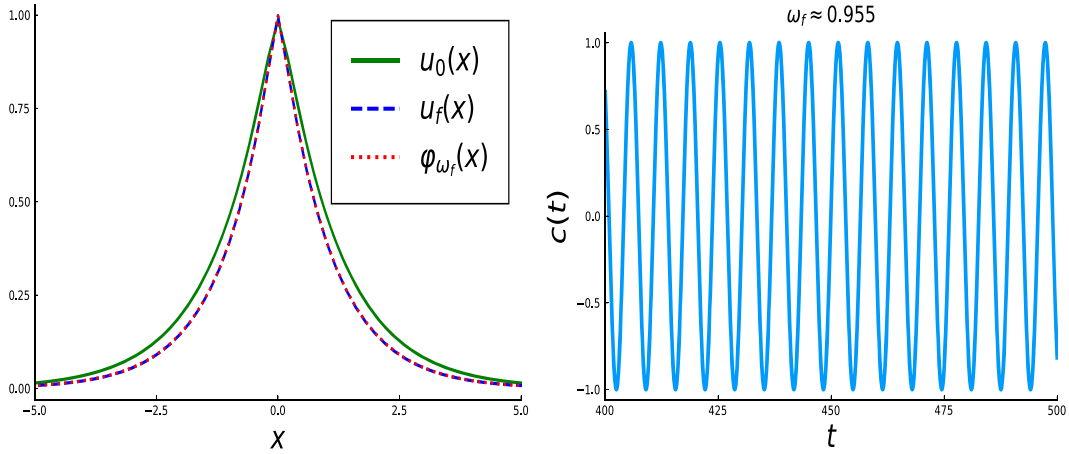

FIG. 8. Left: the initial and final solution profiles of the computations for the transition $B_0 \to B_1$ in Fig. 7 together with the final soliton profile. Right: oscillations near the stable profile for the final segment of numerical computations.

Resorting to numerical computations, we have shown that the smooth bright solitons are spectrally stable for a wide range of parameters and unstable in a narrow interval of frequencies. The latter were indeed checked and identified as pertaining to spectrally unstable solutions. Once the relevant frequency interval and its stability had been mapped, we explored the nonlinear dynamics, not only confirming our dynamical instability findings but also examining the dynamical outcomes of stable solitary waves, upon perturbations of larger amplitudes.

Naturally, these findings raise a number of additional questions that are worthy of further investigation. In the present setting, we only explored individual solitary waves. Yet, it would be quite interesting to examine how the presence of IDD affects the interaction between different solitary waves. This would not only be interesting in the standard case of smooth solitary waves, but also in the limit of $\omega \to 1$ where the profiles of bright solitons become peaked.

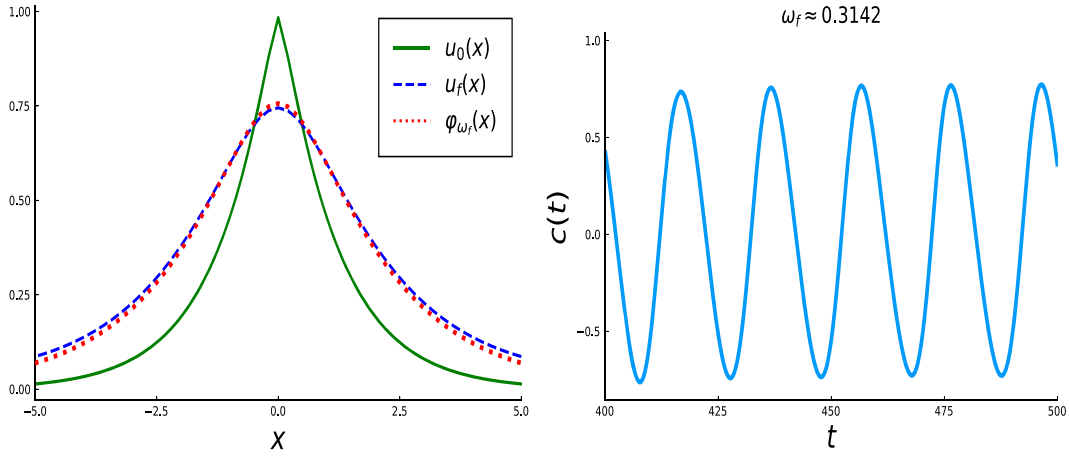

FIG. 9. The same as Fig. 8 but for the transition $B_0 \to B_2$ in Fig. 7.

Furthermore, the vast majority of studies concerning IDD have been limited to one-dimensional realms. Nevertheless, it would be particularly useful to explore the interplay of such IDD features with, e.g. radially symmetric solutions in higher dimensions and indeed not only in just the ones involving standard single-humped solitary waves, but also in more complex settings involving vortices.

Funding

This material is based upon work supported by the U.S. National Science Foundation under the a wards PHY-2110030 and DMS-2 204702 (PGK).

Conflicts of interest

The authors declare no conflict of interest.

Data availability

The authors declare that the data supporting the findings of this study are available within the paper.

REFERENCES

ALBERT, J. & ARBUNICH, J. (2024) Stability of bound states for regularized nonlinear Schrödinger equation. *Stud. Appl. Math.*, **153**, e12780 (37 pages).

ANTONELLI, P., ARBUNICH, J. & SPARBER, C. (2019) Regularizing nonlinear Schrödinger equations through partial off-axis variations. *SIAM J. Math. Anal.*, **51**, 110–130.

CAI, D., BISHOP, A. R. & GRØNBECH-JENSEN, N. (1995) Perturbation theories of a discrete, integrable nonlinear Schrödinger equation. *Phys. Rev. E*, **53**, 4131–4136.

CHANG, J.-H., LIN, C.-Y. & LEE, R.-K. (2022) Quantum harmonic oscillators with nonlinear effective masses in the weak density approximation. *Phys. Scr.*, **97**, 025205.

Comech, A. & Pelinovsky, D. (2003) Purely nonlinear instability of standing waves with minimal energy. *Commun. Pure Appl. Math.*, **56**, 1565–1607.

Dumas, E., Lannes, D. & Szeftel, J. (2016) Variants of the focusing NLS equation: Derivation, justification, and open problems related to filamentation. In: Bandrauk, A., Lorin E., Moloney, J. (eds) *Laser Filamentation*. Cham: Springer International Publishing, pp. 19–75.

Feola, T., Grébert, B. & Iandoli, F. (2023) Long time solutions for quasilinear Hamiltonian perturbations of Schrödinger and Klein-Gordon equations on tori. *Anal. PDE*, **16**, 1133–1203.

Fibich, G. (2015) *The Nonlinear Schrödinger Equation: Singular Solutions and Optical Collapse*. Cham: Springer.

Greentree, A. D., Richards, D., Vaccaro, J. A., Durant, A. V., de Echaniz, S. R., Segal, D. M. & Marangos, J. P. (2003) Intensity-dependent dispersion under conditions of electromagnetically induced transparency in coherently prepared multistate atoms. *Phys. Rev. A*, **67**, 023818.

Ifrim, M. & Tataru, D. (2023) Global solutions for 1d cubic dispersive equations, part III: The quasilinear Schrödinger flow arXiv: 2306.00570.

Johansson, M., Gaididei, Y. B., Christiansen, P. L. & Rasmussen, K. Ø. (1998) Switching between bistable states in a discrete nonlinear model with long-range dispersion. *Phys. Rev. E*, **57**, 4739–4742.

Kenig, C. E., Ponce, G. & Vega, L. (2004) The Cauchy problem for quasi-linear Schrödinger equations. *Invent. Math.*, **158**, 343–388.

Kivshar, Y. S. & Agrawal, G. P. (2003) *Optical Solitons: From Fibers to Photonic Crystals*. San Diego: Academic Press.

Koser, A. A., Sen, P. K. & Sen, P. (2009) Effect of intensity dependent higher-order dispersion on femtosecond pulse propagation in quantum well waveguides. *J. Modern Opt.*, **56**, 1812–1818.

Lin, C. Y., Chang, J. H., Kurizki, G. & Lee, R. K. (2020) Solitons supported by intensity-dependent dispersion. *Opt. Lett.*, **45**, 1471–1474.

Malomed, B. A. & Weinstein, M. I. (1996) Soliton dynamics in the discrete nonlinear Schrödinger equation. *Phys. Lett. A*, **220**, 91–96.

Marzuola, J. L., Metcalfe, J. & Tataru, D. (2021) Quasilinear Schrödinger equations III: Large data and short time. *Arch. Ration. Mech. Anal.*, **242**, 1119–1175.

Mithun, T., Maluckov, A., Mančić, A., Khare, A. & Kevrekidis, P. G. (2023) How close are integrable and nonintegrable models: A parametric case study based on the Salerno model. *Phys. Rev. E*, **107**, 024202 (9 pages).

Kevrekidis, P. G., Frantzeskakis, D. J. & Carretero-González, R. (2015) *The Defocusing Nonlinear Schrödinger Equation: From Dark Solitons to Vortices and Vortex Rings*. Philadelphia, PA: Society for Industrial and Applied Mathematics.

Pelinovsky, D. E., Afanasjev, V. V. & Kivshar, Y. S. (1996) Nonlinear theory of oscillating, decaying, and collapsing solitons in the generalized nonlinear Schrödinger equation. *Phys. Rev. E*, **53**, 1940–1953.

Pelinovsky, D. E. & Plum, M. (2024a) Stability of black solitons in optical systems with intensity-dependent dispersion. *SIAM J. Math. Anal.*, **56**, 2521–2568.

Pelinovsky, D. E. & Plum, M. (2024b) Dynamics of black solitons in a regularized nonlinear Schrodinger equation. *Proceedings AMS*, **152**, 1217–1231.

Pelinovsky, D. E., Ross, R. M. & Kevrekidis, P. G. (2021) Solitary waves with intensity-dependent dispersion: Variational characterization. *J. Phys. A: Math. Theor.*, **54**, 445701 (15 pages).

Pitaevskii, L. P. & Stringari, S. (2003) *Bose-Einstein Condensation*. Oxford: Oxford University Press.

Poppenberg, M. (2001) Smooth solutions for a class of fully nonlinear Schrödinger type equations. *Nonlinear Anal.*, **45**, 723–741.

Ross, R. M., Kevrekidis, P. G. & Pelinovsky, D. E. (2021) Localization in optical systems with an intensity-dependent dispersion. *Q. Appl. Math.*, **79**, 641–665.

Salerno, M. (1992) Quantum deformations of the discrete nonlinear Schrödinger equation. *Phys. Rev. A*, **46**, 4856–4859.

Veltz, R. (2020) *BifurcationKit.Jl* URL: https://hal.archives-ouvertes.fr/hal-02902346.